OPEN

Noise Intensity-Intensity Correlations and the Fourth Cumulant of Photo-assisted Shot Noise

Jean-Charles Forgues[1], Fatou Bintou Sane[1], Simon Blanchard[2], Lafe Spietz[3], Christian Lupien[1] & Bertrand Reulet[1]

[1]Département de Physique, Université de Sherbrooke, Sherbrooke, Québec, Canada, J1K 2R1, [2]Département de Génie électrique, Université de Sherbrooke, Sherbrooke, Québec, Canada, J1K 2R1, [3]National Institute of Standards and Technology, Boulder, Colorado 80305, USA.

We report the measurement of the fourth cumulant of current fluctuations in a tunnel junction under both dc and ac (microwave) excitation. This probes the non-Gaussian character of photo-assisted shot noise. Our measurement reveals the existence of correlations between noise power measured at two different frequencies, which corresponds to two-mode intensity correlations in optics. We observe positive correlations, *i.e.* photon bunching, which exist only for certain relations between the excitation frequency and the two detection frequencies, depending on the dc bias of the sample.

In mesoscopic physics, a lot of effort has been put in the measurement and understanding of current fluctuations[1,2]. Of particular interest are the deviations from the ubiquitous Gaussian noise, *i.e.* the study of high order cumulants. As a matter of fact, while the only parameter characterizing a Gaussian distribution, the variance or *second cumulant* of the fluctuations, contains some information about electron transport, much more could be learned by the statistical study of the fluctuations beyond their variance. These are characterized by cumulants of order three and higher, which are zero for a Gaussian distribution. For the simplest systems, such as a tunnel junction between normal metals or a quantum point contact, only the third cumulant has been measured until now[3–6]. Higher order cumulants have been experimentally accessible solely in quantum dots where electrons enter only one by one[7–9]. In all these measurements the system is driven out of equilibrium by a dc voltage bias. Here we address the statistics of photo-assisted shot noise, *i.e.* current fluctuations in the presence of an ac excitation. While the variance of such fluctuations has been well explored both theoretically[10–13] and experimentally[14–19], no experiment has been performed yet that reports the existence of higher order cumulants in such conditions.

In the following we present a link between the measurement of the correlation $G_2 = \langle P_1 P_2 \rangle - \langle P_1 \rangle \langle P_2 \rangle$ between the noise powers P_1 and P_2 at two different frequencies in the GHz range, f_1 and f_2. The source of shot noise is a tunnel junction that is dc biased and excited at frequency f_0. Since power fluctuations of Gaussian noise are independent at all frequencies, our measurement probes only the non-Gaussian part of current fluctuations. This technique has been applied many times to the study of 1/f noise in glassy or disordered materials[20–23] and has been proposed to measure the fourth cumulant of a quantum point contact without ac excitation[24]. In optics, G_2 corresponds to intensity-intensity correlations, a usual probe of the statistical properties of light[25]. Here we show that G_2 gives the fourth cumulant at frequencies $(f_1, f_2, 0)$ of photo-assisted shot noise in the tunnel junction. In the optics community, current/voltage fluctuations, which are simply another point of view of a fluctuating electromagnetic field, are rather thought of as time dependent electric and magnetic fields. Thus, a noisy electronic device is also a light source, and it is natural to apply tools developed in optics to analyze high frequency electronic noise[24,26,27]. This point of view will also be studied.

Results

Experimental principle. The experimental setup is depicted on Fig. 1. The sample, a tunnel junction described in the *Methods* section, is voltage biased by a dc source and connected to microwave signal generators below 4 GHz and above 8 GHz while the noise generated by the junction at point A is amplified by a cryogenic amplifier in the 4–8 GHz frequency range. This setup allows noise to be measured in the 4–8 GHz range while the excitation frequency f_0 can take any value below 4 GHz or above 8 GHz. This insures that the amplifier never sees the ac
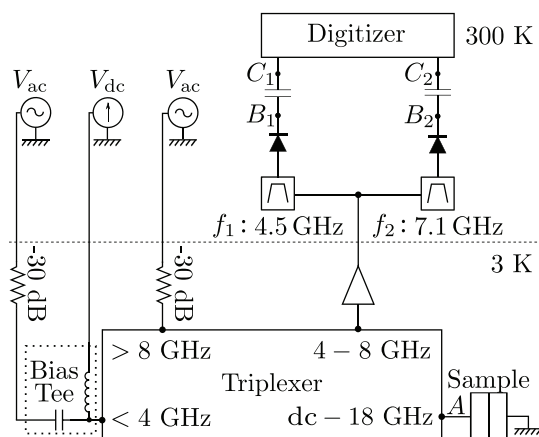
Figure 1 | Experimental setup. Diode symbols represent fast power detectors.

excitation of the sample, which avoids spurious signals due to non-linearities in the amplifier at high excitation power. However, it prevents the use of an excitation frequency in the range 4–8 GHz.

The amplified noise is split into two branches: in branch 1 (respectively branch 2) the signal is bandpass filtered around $f_1 = 4.5$ GHz with a bandwidth $\Delta f_1 = 0.72$ GHz (resp. $f_2 = 7.1$ GHz, $\Delta f_2 = 0.60$ GHz). In each branch a fast power detector (diode symbol on Fig. 1, bandwidth $\Delta \varepsilon \simeq 100$ MHz) measures the "instantaneous" (averaged over a few ns) noise power integrated in the corresponding bandwidth, i.e. $v_{B_k}(t) \propto P_k(t)$ with $k = 1, 2$. The dc voltage at point B_k is thus proportional to the noise spectral density, $S(f_k) = \langle |i(f_k)|^2 \rangle$ with $i(f)$ the Fourier component of the instantaneous current: $\langle v_{B_k} \rangle \propto S(f_k) \Delta f_k$. A dc block (capacitor on Fig. 1) removes the dc part of v_B to give $v_{C_k}(t) \propto P_k(t) - \langle P_k \rangle = \delta P_k(t)$. Finally, voltages at points C_1 and C_2 are simultaneously digitized with a 2-channel, 14-bit, 400 MS/s acquisition card and the correlator $G_2 = \langle \delta P_1 \delta P_2 \rangle$ is computed in real time by a 12-core parallel computer, as are the auto-correlations of both channels $\langle \delta P_k^2 \rangle$.

The fourth cumulant of noise. In order to describe and understand the meaning of the observed correlator, let us first express the noise generated by the sample in Fourier space. We define the power fluctuations $\delta P_k(t) = P_k(t) - \langle P_k \rangle$ so that $G_2 = \langle \delta P_1(t) \delta P_2(t) \rangle$. The average $\langle . \rangle$ is performed over time. Introducing the Fourier component of the power fluctuations $\delta P_k(\varepsilon)$ at frequency ε, one has: $G_2 = \int d\varepsilon \langle \delta P_1(\varepsilon) \delta P_2(-\varepsilon) \rangle$. Here ε is a low frequency limited by the output bandwidth of the power detectors. Note that $\delta P_k(\varepsilon = 0) = 0$, while power fluctuations at finite frequency ε are related to current fluctuations by $\delta P_k(\varepsilon \neq 0) \propto \int df [i(f)i(\varepsilon - f) + i(-f)i(\varepsilon + f)]$ where $i(f)$ is the fluctuating current's Fourier component at frequency f. This integral spans over the bandwidth of the bandpass filters, i.e. $f_k \pm \Delta f_k/2$. Thus, G_2 is proportional to the correlator between currents at four *different* frequencies which, by definition, is the time averaged fourth *cumulant* of current fluctuations taken at frequencies f_1, f_2 and ε (with $\varepsilon \to 0$ but $\varepsilon \neq 0$).

$$G_2 \propto \langle i(f_1)i(\varepsilon - f_1)i(f_2)i(-\varepsilon - f_2) \rangle \Delta f_1 \Delta f_2 \Delta \varepsilon \qquad (1)$$

Noting $i_k(t)$ the current after bandpass filtering around $\pm f_k$, one has $G_2 \propto \langle\langle (i_1 + i_2)^4(t) \rangle\rangle - \langle\langle i_1^4(t) \rangle\rangle - \langle\langle i_2^4(t) \rangle\rangle$, the averaging being performed over the time t. Here $\langle\langle x^4 \rangle\rangle = \langle x^4 \rangle - 3\langle x^2 \rangle^2$ is the fourth cumulant of the random variable x with $\langle x \rangle = 0$. For a Gaussian distribution, $\langle\langle x^4 \rangle\rangle = 0$, so there is no information in the fourth moment that is not contained in the variance. In contrast, for a non-Gaussian distribution, the fourth moment differs from $3\langle x^2 \rangle^2$, though only very slightly for current fluctuations involving many electrons, so the fourth cumulant is non-zero.

Frequency dependence. The first step in the observation of $G_2(V_{dc}, V_{ac}, f_0)$ is to determine the excitation frequency for which $G_2 \neq 0$. This is done by measuring G_2 at fixed bias voltage ($V_{dc} = 0$ or $V_{dc} = 2.4$ mV) and fixed excitation amplitude ($V_{ac} = 1.1$ mV) while varying the excitation frequency f_0 from 10 MHz to 3.83 GHz and from 10 GHz to 14 GHz. These results are reported in Fig. 2, where G_2 has been reduced to units of K^2 as the measured noise spectral density S of a conductor of resistance R is often given in terms of equivalent noise temperature $T_{noise} = RS/2k_B$. We observe that G_2 is large at low frequency for both bias voltages. This simply reflects that a slow oscillation of the bias voltage induces a slow modulation of the noise, i.e. a slow oscillation of both P_1 and P_2. The response disappears when the modulation frequency exceeds the output bandwidth of the power detectors.

At much higher excitation frequencies, G_2 strongly depends on V_{dc}. For $V_{dc} = 2.4$ mV, G_2 shows peaks at $f_0 = 2.6$ GHz and $f_0 = 11.6$ GHz, which correspond to $f_\mp = f_2 \mp f_1$, where f_1 and f_2 are the signal observation frequencies. At zero bias, G_2 peaks at $f_0 = 1.3$ GHz, or $f_-/2$. Choosing $f_0 = f_+/2$ was not possible with this experimental setup since it lies in the 4–8 GHz range.

To understand why G_2 is nonzero at high excitation frequency, let us first consider the correlator $\langle i(f)i(f') \rangle$. The latter is non-vanishing only for frequencies such that $f + f' = nf_0$ with n, an integer. The case $n = 0$ corresponds to photo-assisted noise whereas $n \neq 0$ describes the noise dynamics, characterized by the correlator $X_n(f, f_0) = \langle i(f)i(nf_0 - f) \rangle$[17,28,29]. In order to detect the fourth cumulant and not the fourth moment of current fluctuations, it is crucial that the four frequencies involved in G_2 (see Eq. 1 where $\varepsilon \neq 0$) be different so that correlators $\langle i(f)i(-f) \rangle$ are never involved. Experimentally, the separation of the signal into two branches with non-overlapping bandwidths insures that $f_1 \neq \pm f_2$, while the presence of the dc blocks, by imposing $\varepsilon \neq 0$, prevents all other possible occurrences of such correlators. In our experimental setup, relevant frequencies are close to $\pm f_1$ and $\pm f_2$, so this condition becomes $f_1 \pm f_2 = nf_0$, i.e. $f_0 = f_\pm/n$. In such cases, the fourth order correlator of Eq. (1) is dominated by the terms $\langle i(f_1)i(\pm f_2) \rangle \langle i(-f_1)i(\mp f_2) \rangle$. This product is zero unless $f_1 \pm f_2 = nf_0$, as we observe on Fig. 2.

Voltage dependence. We now consider the variation of G_2 as a function of the dc voltage for various ac excitation amplitudes at fixed excitation frequency $f_0 = f_\pm/n$. Data on Fig. 3 correspond to an excitation at $f_0 = f_+$. We observe that G_2 is maximal at high dc bias and vanishes at $V_{dc} = 0$. We obtained identical results for $f_0 = f_-$ (data not shown). Data on Fig. 4 correspond to $f_0 = f_-/2$. Here G_2 peaks at 0 dc bias and decays when $|V_{dc}|$ increases. Moreover, the
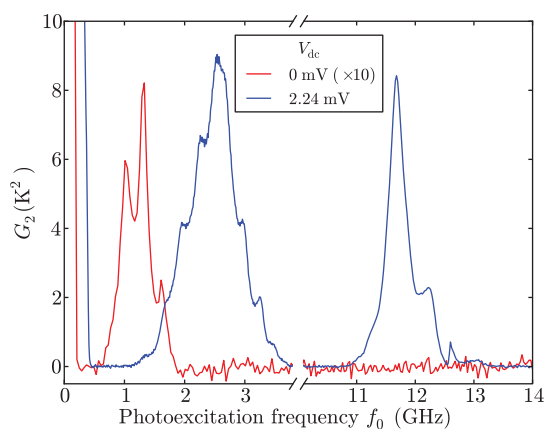

Figure 2 | Reduced G_2 vs excitation frequency f_0 for two bias voltages: V_{dc} = 0 (in red) and $V_{dc} = 2.24$ mV (in blue). The ac excitation amplitude is $V_{ac} = 1.1$ mV for both measurements. The exact shape of the peaks is determined by the frequency response of the experimental setup.
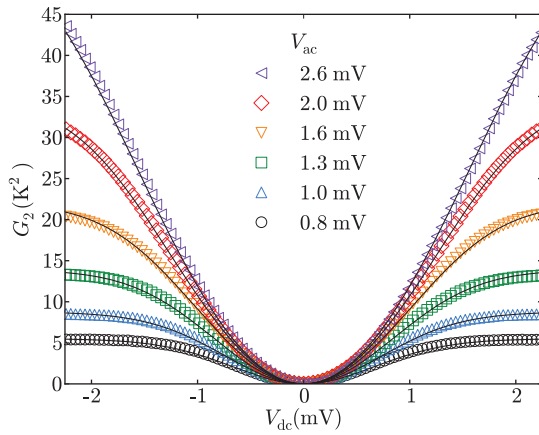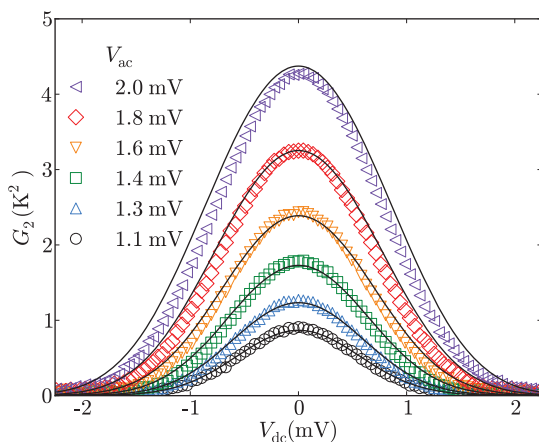
2

Figure 3 | Reduced G_2 vs dc bias voltage for various ac excitation amplitudes at frequency $f_0 = f_+ = 11.6$ GHz. Symbols are experimental data and solid lines theoretical expectations of Eq. (2) and (3).

maximum of $G_2(f_0 = f_\pm)$ for a given V_{ac} is an order of magnitude larger than that of $G_2(f_0 = f_-/2)$.

The voltage dependence of the signal can be explained by expressing G_2 in terms of the correlators $X_n(f, f_0)$:

$$G_2(f_0 = f_\pm/n) = K|X_n(f_1, f_0)|^2 \qquad (2)$$

with $K \simeq 4\Delta f_1 \Delta f_2$. The exact value of K involves integrals of the gain of the setup over the actual bandwidth of the filters as well as the coupling coefficient between the sample and the detection setup, which depends on the impedance of the sample. The correlators X_n have been calculated and measured in the quantum regime at very low temperature[17,28,29]. In the high temperature, classical regime that corresponds to the present experiment, X_n reduces to:

$$X_n = \int_{-\pi}^{\pi} S_0(V_{dc} + V_{ac}\cos\theta)\exp(in\theta)\frac{d\theta}{2\pi} \qquad (3)$$

Here $S_0(V) = 2\,eGV\coth(eV/2k_BT)$ is the noise of the junction at zero frequency in the absence of ac excitation. Eq. 3 is interpreted as follows: in the classical regime, the noise responds instantaneously to the time-dependent voltage $V(t) = V_{dc} + V_{ac}\cos\theta$ with $\theta = 2\pi f_0 t$, so it oscillates at frequency f_0 and its harmonics. X_n is the amplitude of the nth harmonics. X_n is independent of f and f_0 as long as hf, $hf_0 \ll k_BT$, so $G_2(f_0 = f_\pm/n) = KX_n^2$ depends only on $|n|$.

For small V_{ac} and $f_0 = f_\pm$, the noise oscillates with an amplitude given by $X_1 \propto V_{ac}\frac{dS_0}{dV}$, so $G_2 = KX_1^2$ computes to zero at $V_{dc} = 0$ and is maximal at large V, which corresponds to the shape observed on Fig. 3. For $f_0 = f_\pm/2$, G_2 is given by the amplitude of the noise that oscillates at $2f_0$, which is given by $X_2 \propto \frac{d^2S_0}{dV^2}V_{ac}^2$ for small V_{ac}. Therefore $G_2 = KX_2^2$ is maximal at $V_{dc} = 0$ and decays at finite dc bias, as observed on Fig. 4. Solid lines on Fig. 3 and 4 represent the theoretical predictions of Eqs. (2,3) and agree very well with the measurements.

Photon bunching. Current fluctuations generated by a tunnel junction are known to be non-Gaussian, and thus should exhibit a non-zero fourth cumulant even in the absence of ac excitation[30]. This contribution, together with potential environmental effects[31,32] are negligible as compared to the signals we report here. For example, at $V_{dc} = 2$ mV and $V_{ac} = 0$, the correlator would correspond to $G_2 \sim 10^{-4}$ K². Thus, by adding an ac excitation on the sample we have been able to boost the fourth cumulant by 5 orders of magnitude.

Furthermore, our experiment corresponds to intensity-intensity correlation, which is the usual way used to differentiate classical from quantum light by showing evidence of photon bunching or anti-bunching. More precisely, in order to make a connection with experiments performed in optics, let us define the dimensionless correlator:

$$g_2 = \frac{\langle P_1 P_2 \rangle}{\langle P_1 \rangle \langle P_2 \rangle} = 1 + \frac{G_2}{\langle P_1 \rangle \langle P_2 \rangle} \qquad (4)$$

which is usually referred to as the same-time two-mode second order correlator of the electromagnetic field radiated by the junction.

The variations of g_2 as a function of V_{dc} are depicted on Fig. 5 for fixed $V_{ac} = 1.0$ mV for both $f_0 = f_+$ (red triangles) and $f_0 = f_-/2$ (green circles). It is clear from these data that we always observe a positive correlation between the power fluctuations, i.e. photon bunching ($g_2 > 1$). Each acquisition performed by the digitizer (integrated over $\tau = 2.5$ ns) corresponds to an averaged number of $\langle n_2 \rangle = P_2\tau/hf_2 \sim 21$ photons at 7.2 GHz emitted by the sample at $V_{dc} = V_{ac} = 1$ mV and $f_0 = f_+$, plus ~40 photons from the amplifier. Thus our experiment does not measure correlations at the single photon level, but is not very far from that limit, which can be reached by lowering the temperature and the ac power.
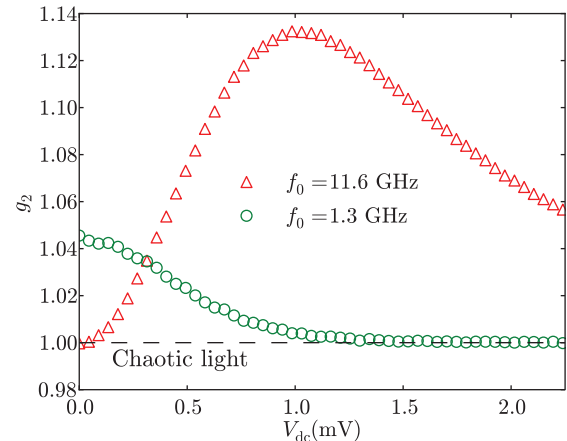

Figure 4 | Reduced G_2 vs dc bias voltage for various ac excitation amplitudes at frequency $f_0 = f_-/2 = 1.3$ GHz. Symbols are experimental data and solid lines theoretical expectations of Eq. (2) and (3).

Figure 5 | Measured g_2 vs dc bias voltage at $V_{ac} = 1.0$ mV for an excitation frequency $f_0 = f_+$ (red triangles) or $f_0 = f_-/2$ (green circles). The dashed line at $g_2 = 1$ represents independent photons, i.e. chaotic light, while $g_2 > 1$ corresponds to photon bunching.

Discussion

It follows from the observed behaviour that by choosing the excitation frequency, dc bias and ac excitation, we can control how non-Gaussian the shot noise of the junction can be. The level of non-Gaussianity of the signal is characterised here by the fourth cumulant, which is directly linked to the measured correlator.

It should be noted that the power detector, which measures the square of the electric field, cannot differentiate absorption from emission of photons by the sample. This has to be taken into account when comparing the data with theories such as[24,26,27] which consider photon detectors. In particular, the correlations between photon detectors will involve other current correlators[33]. Whereas G_2 at excitation frequency $f_0 = f_1 + f_2$ corresponds to absorption of one photon of frequency f_0 and emission of two correlated photons, one at f_1 and one at f_2, the case of excitation at frequency $f_0 = f_2 - f_1$ corresponds to two photons being absorbed, one at f_0 and one at f_1 while one photon at frequency f_2 is emitted. We indeed observe no difference in G_2 for $f_0 = f_+$ and $f_0 = f_-$.

The tunnel junction behaves as a source of white noise whose amplitude is instantaneously modulated by the bias voltage. This description holds only because the temperature is large in the present experiment. At very low temperature, the noise can no longer be considered as white and no longer responds adiabatically to an ac excitation, so Eq.(3) will no longer be valid. In particular, X_n depends on f and f_0, so that excitations at $f_1 + f_2$ or $f_1 - f_2$ will no longer correspond to the same G_2. Still the present analysis, and in particular the link between G_2 and X_n given by Eq.(2), will remain valid. Our measurements open the way to the study of the fourth cumulant of current fluctuations in the quantum regime at very low temperature, where the same setup can be used to detect correlations at the single photon level.

Methods

Sample. We have chosen to perform the measurement on the simplest system that exhibits well understood shot noise, the tunnel junction. The sample is a ~1 μm × 15 μm Al/Al oxide/Al tunnel junction made by photolithography, similar to that used for noise thermometry[34], cooled at $T = 3.0$ K so the aluminum remains a normal metal. The resistance of the junction at that temperature, $R = 22\,\Omega$, is close enough to the 50 Ω impedance of the microwave circuitry to ensure a good coupling. The capacitance of the junction corresponds to an RC frequency cutoff of ~6 GHz, so it influences the amplitude of the noise we measure and the amplitude of the ac excitation experienced by the junction. Both effects are calibrated out as explained below.

Calibration. In order to have a quantitative measurement of G_2, it is necessary to calibrate the ac excitation voltage reaching the sample and the overall gain of the detection. The calibration of the ac voltage across the sample is performed by measuring the usual photo-assisted noise, *i.e.* S vs V_{dc}, in the presence of a microwave excitation for various excitation voltages[10,14]. The temperature is large enough ($k_B T \gg h f_{1,2}$) to approximate the noise measured in either branch by its value at zero frequency. In the absence of ac excitation, the noise spectral density is given by $S_0(V_{dc}) = eGV_{dc} \coth(eV_{dc}/2k_B T)$ with $G = 1/R$, the sample's conductance. Since the excitation frequency f_0 is always such that $h f_0 \ll k_B T$, the photo-assisted noise can be approximated by its time-average value as if the junction were responding instantaneously to the time-dependent voltage. To calibrate the gain of the setup, we consider the single channel autocorrelations $\langle \delta P_k^2 \rangle$. Those are also related to fourth order current correlators $\langle i(f) i(\varepsilon - f) i(f') i(-\varepsilon - f') \rangle$. However, here f and f' belong to the same frequency band, so the correlator is dominated by terms $f = -f'$, and $\langle \delta P_k^2 \rangle \propto \langle P_k \rangle^2$. The fourth cumulant G_2 is only a very small correction to this. Thus, power correlations within the same frequency band are totally dominated by Gaussian fluctuations, as in[35]. Note that since the amplifier noise dominates $\langle P_k \rangle$, it also dominates $\langle \delta P_k^2 \rangle$, but only the fourth cumulant of the amplifier's noise contributes to G_2 (here a very small contribution).

1. Blanter, Y. M. & Büttiker, M. Shot noise in mesoscopic conductors. *Phys. Rep.* **336**, 1–166 (2000).
2. Nazarov, Y. V. & Blanter, Y. M. *Quantum Noise In Mesoscopic Physics.* Nato Science Series vol. II/97, Kluwer Academic Publishers (2009).
3. Reulet, B., Senzier, J. & Prober, D. E. Environmental effects in the third moment of voltage fluctuations in a tunnel junction. *Phys. Rev. Lett.* **91**, 196601 (2003).
4. Bomze, Y., Gershon, G., Shovkun, D., Levitov, L. S. & Reznikov, M. Measurement of counting statistics of electron transport in a tunnel junction. *Phys. Rev. Lett.* **95**, 176601 (2005).
5. Gershon, G., Bomze, Y., Sukhorukov, E. V. & Reznikov, M. Detection of non-gaussian fluctuations in a quantum point contact. *Phys. Rev. Lett.* **101**, 016803 (2008).
6. Gabelli, J. & Reulet, B. High frequency dynamics and the third cumulant of quantum noise. *J. Stat. Mech.* P01049 (2009).
7. Gustavsson, S. *et al.* Counting statistics of single electron transport in a quantum dot. *Phys. Rev. Lett.* **96**, 076605 (2006).
8. Gustavsson, S. *et al.* Measurements of higher-order noise correlations in a quantum dot with a finite bandwidth detector. *Phys. Rev. B* **75**, 075314 (2007).
9. Flindt, C. *et al.* Universal oscillations in counting statistics. *Proc. Natl. Acad. Sci. USA* **106**, 10116 (2009).
10. Lesovik, G. B. & Levitov, L. S. Noise in an ac biased junction: nonstationary Aharonov-Bohm effect. *Phys. Rev. Lett.* **72**, 538 (1994).
11. Vanevic, M., Nazarov, Y. V. & Belzig, W. Elementary events of electron transfer in a voltage-driven quantum point contact. *Phys. Rev. Lett.* **99**, 076601 (2007).
12. Vanevic, M., Nazarov, Y. V. & Belzig, W. Elementary charge-transfer processes in mesoscopic conductors. *Phys. Rev. B* **78**, 245308 (2008).
13. Vanevic, M. & Belzig, W. Control of electron-hole pair generation by biharmonic voltage drive of a quantum point contact. *Phys. Rev. B* **86**, 241306 (2012).
14. Schoelkopf, R. J., Kozhevnikov, A. A. & Prober, D. E. Observation of "photon-assisted" shot noise in a phase-coherent conductor. *Phys. Rev. Lett.* **80**, 2437 (1998).
15. Kozhevnikov, A. A., Schoelkopf, R. J. & Prober, D. E. Observation of Photon-Assisted Noise in a Diffusive Normal Metal-Superconductor Junction. *Phys. Rev. Lett.* **84**, 3398 (2000).
16. Reydellet, L.-H., Roche, P., Glattli, D. C., Etienne, B. & Jin, Y. Quantum partition noise of photon-created electron-hole Pairs. *Phys. Rev. Lett.* **90**, 176803 (2003).
17. Gabelli, J. & Reulet, B. Dynamics of quantum noise in a tunnel junction under ac excitation. *Phys. Rev. Lett.* **100**, 026601 (2008).
18. Gabelli, J. & Reulet, B. Shaping a time-dependent excitation to minimize the shot noise in a tunnel junction. *Phys. Rev. B* **87**, 075403 (2013).
19. Gasse, G., Spietz, L., Lupien, C. & Reulet, B. Observation of quantum oscillations in the photo-assisted shot noise of a tunnel junction. arXiv1304.6951 (unpublished).
20. Restle, P. J., Weissman, M. B. & Black, R. D. Tests of Gaussian statistical properties of 1/f noise. *J. Appl. Phys.* **54**, 5844 (1983).
21. Weissman, M. B. 1/f noise and other slow, nonexponential kinetics in condensed matter. *Rev. Mod. Phys.* **60**, 537 (1988).
22. Parman, C. E., Israeloff, N. E. & Kakalios, J. Conductance-noise power fluctuations in hydrogenated amorphous silicon. *Phys. Rev. Lett.* **69**, 1097 (1992).
23. Weissman, M. B. What is a spin glass? A glimpse via mesoscopic noise. *Rev. Mod. Phys.* **65**, 829 (1993).
24. Lebedev, A. V., Lesovik, G. B. & Blatter, G. Statistics of radiation emitted from a quantum point contact. *Phys. Rev. B* **81**, 155421 (2010).
25. Loudon, R. *The Quantum Theory of Light.* Oxford University Press, Third edition (2000).
26. Beenakker, C. W. J. & Schomerus, H. Counting statistics of photons produced by electronic shot noise. *Phys. Rev. Lett.* **86**, 700 (2001).
27. Beenakker, C. W. J. & Schomerus, H. Antibunched photons emitted by a quantum point contact out of equilibrium. *Phys. Rev. Lett.* **93**, 096801 (2004).
28. Gabelli, J. & Reulet, B. The noise susceptibility of a photo-excited coherent conductor. arXiv:0801.1432 (unpublished).
29. Gabelli, J. & Reulet, B. The noise susceptibility of a coherent conductor. *Proceedings of SPIE, Fluctuations and Noise in Materials*, 6600 (2007).
30. Levitov, L. S., Lee, H. W. & Lesovik, G. B. Electron counting statistics and coherent states of electric current. *J. Math. Phys.* **37**, 4845–4866 (1996).
31. Beenakker, C. W. J., Kindermann, M. & Nazarov, Y. V. Temperature-dependent third cumulant of tunneling noise. *Phys. Rev. Lett.* **90**, 176802 (2003).
32. Kindermann, M., Nazarov, Y. V. & Beenakker, C. W. J. Feedback of the electromagnetic environment on current and voltage fluctuations out of equilibrium. *Phys. Rev. B* **69**, 035336 (2004).
33. Bednorz, A. & Belzig, W. Models of mesoscopic time-resolved current detection. *Phys. Rev. B* **81**, 125112 (2010).
34. Spietz, L., Lehnert, K. W., Siddiqi, I. & Schoelkopf, R. J. Primary electronic thermometry using the shot noise of a tunnel junction. *Science* **300**, 1929–1932 (2003).
35. Zakka-Bajjani, E. *et al.* Experimental determination of the statistics of photons emitted by a tunnel junction. *Phys. Rev. Lett.* **104**, 206802 (2010).

Acknoledgments

Author contributions

J.-C.F. and F.B.S. performed the measurements and data analysis, S.B. designed and implemented the real-time digital correlator, L.S. fabricated the samples, C.L. designed and programmed the control of the experiments. B.R. designed the experiment and performed the theory. B.R. and C.L. supervised the measurements. The article was mainly written by J.-C.F. and B.R.

Additional information